Cancer Science
Japanese Cancer Association JCA
Open Access

Regulation of spindle and kinetochore-associated protein 1 by antitumor *miR-10a-5p* in renal cell carcinoma

Takayuki Arai,[1,2] Atsushi Okato,[1,2] Satoko Kojima,[3] Tetsuya Idichi,[4] Keiichi Koshizuka,[1] Akira Kurozumi,[1,2] Mayuko Kato,[1,2] Kazuto Yamazaki,[5] Yasuo Ishida,[5] Yukio Naya,[3] Tomohiko Ichikawa[2] and Naohiko Seki[1]

Departments of [1]Functional Genomics; [2]Urology, Chiba University Graduate School of Medicine, Chiba; [3]Department of Urology, Teikyo University Chiba Medical Center, Ichihara; [4]Department of Digestive Surgery, Breast and Thyroid Surgery, Graduate School of Medical Sciences, Kagoshima University, Kagoshima; [5]Department of Pathology, Teikyo University Chiba Medical Center, Ichihara, Japan

Key words

MicroRNA, *miR-10a-5p*, renal cell carcinoma, spindle and kinetochore-associated protein 1, tyrosine kinase inhibitor resistance

Correspondence

Naohiko Seki, Department of Functional Genomics, Chiba University Graduate School of Medicine, 1-8-1 Inohana, Chuo-ku, Chiba 260-8670, Japan.
Tel: +81-43-226-2971; Fax: +81-43-227-3442;
E-mail: naoseki@faculty.chiba-u.jp

Funding information

This study was supported by KAKENHI grants 15K10801, 16K20125, and 16H05462.

Received May 22, 2017; Revised July 20, 2017; Accepted July 23, 2017

Cancer Sci **108** (2017) 2088–2101

doi: 10.1111/cas.13331

Analysis of our original microRNA (miRNA) expression signature of patients with advanced renal cell carcinoma (RCC) showed that *microRNA-10a-5p* (*miR-10a-5p*) was significantly downregulated in RCC specimens. The aims of the present study were to investigate the antitumor roles of *miR-10a-5p* and the novel cancer networks regulated by this miRNA in RCC cells. Downregulation of *miR-10a-5p* was confirmed in RCC tissues and RCC tissues from patients treated with tyrosine kinase inhibitors (TKI). Ectopic expression of *miR-10a-5p* in RCC cell lines (786-O and A498 cells) inhibited cancer cell migration and invasion. Spindle and kinetochore-associated protein 1 (*SKA1*) was identified as an antitumor *miR-10a-5p* target by genome-based approaches, and direct regulation was validated by luciferase reporter assays. Knockdown of *SKA1* inhibited cancer cell migration and invasion in RCC cells. Overexpression of SKA1 was observed in RCC tissues and TKI-treated RCC tissues. Moreover, analysis of The Cancer Genome Atlas database demonstrated that low expression of *miR-10a-5p* and high expression of *SKA1* were significantly associated with overall survival in patients with RCC. These findings showed that downregulation of *miR-10a-5p* and overexpression of the *SKA1* axis were highly involved in RCC pathogenesis and resistance to TKI treatment in RCC.

Renal cell carcinoma accounts for approximately 2–5% of adult malignancies worldwide, and approximately 350 000 new cases are diagnosed, with over 140 000 deaths, each year.[1,2] Most cases of RCC (approximately 80%) are classified as ccRCC.[3] In the majority of patients, ccRCC is associated with dysfunction of the *VHL* gene.[4,5] Lack of *VHL* function causes activation of HIF and VEGF pathways in ccRCC cells.[6,7] The mTOR pathway is also activated by dysregulation of HIF and VEGF pathways in patients with ccRCC.[8,9]

Based on this information regarding the molecular pathogenesis of ccRCC, molecular targeted therapies for patients with advanced and metastatic RCC have been developed during the past decade.[10] The molecular-targeted agents sorafenib, sunitinib, pazopanib, axitinib, bevacizumab, and cabozantinib inhibit VEGF and VEGF receptor pathways, and temsirolimus and everolimus inhibit the mTOR pathway; treatment with these agents has resulted in significant benefits to patients with advanced RCC.[10,11] However, the curative effects of these treatments are limited because cancer cells exhibit activation of several alternative signal cascades and acquire resistance to these treatments during therapeutic processes.[11,12] Treatment strategies for drug-resistant cancer cells are limited, and the prognosis of these patients is extremely poor. However, the molecular mechanisms of resistance to molecular-targeted therapies in RCC cells are still unclear.

miRNAs act as pivotal players that regulate the expression control of protein-coding/protein-noncoding RNAs in a sequence-dependent manner.[13,14] Notably, a single miRNA can directly control many mRNAs in human cells.[15] Therefore, aberrantly expressed miRNAs can disrupt the tight control of RNA expression in cancer cells. Moreover, dysregulation of miRNAs is deeply involved in cancer cell progression, metastasis, and drug resistance.[16–19]

In RCC, miRNAs are closely related to the development of cancer, and previous studies have reported the relationships among many miRNAs and RCC. For example, the *miR-200* family, containing *miR-141*, *miR200a/b/c*, and *miR-429*, forms two clusters, *miR-200a/200b/429* and *miR-141/200c*, and expression of the *miR-200* family is markedly downregulated in RCC tissues.[20] Additionally, the *miR-200* family has been reported to be involved in the EMT in several cancers, and *miR-141* and *miR-200c* function as tumor suppressors in RCC by inhibiting the EMT through targeting of *ZFHX1B*, a transcriptional repressor for CDH1/E-cadherin.[20,21] In this way, investigation of molecular networks based on miRNAs may help to elucidate the molecular mechanisms mediating the progression of RCC.

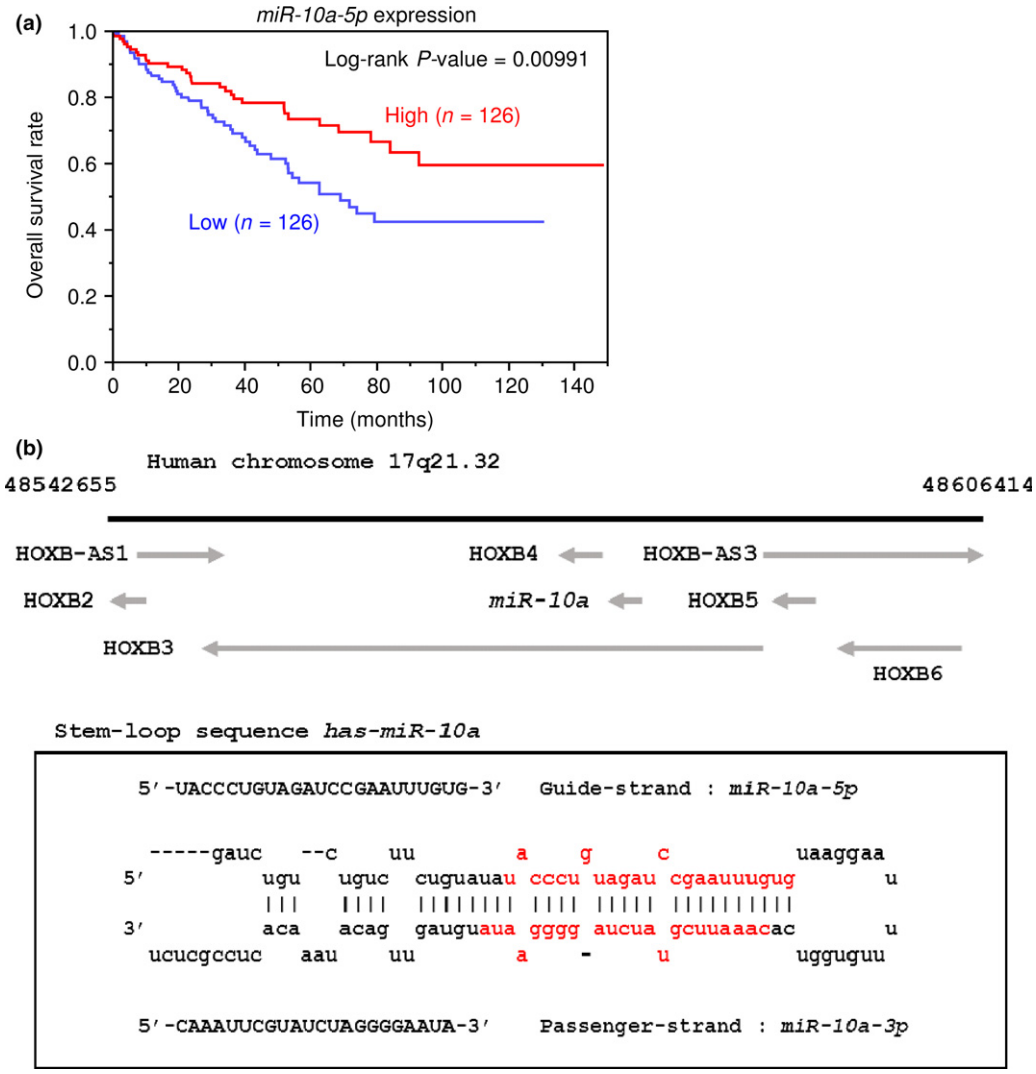

Fig. 1. Kaplan-Meier survival curves based on *miR-10a-5p* expression in patients with clear cell renal cell carcinoma (ccRCC), and schematic representation of the chromosomal location of human *miR-10a*. (a) Kaplan-Meier survival curve for overall survival rate based on *miR-10a-5p* expression in patients with ccRCC from The Cancer Genome Atlas (TCGA) database. (b) *miR-10a* is located on human chromosome 17q21.32. Mature microRNAs (miRNAs), *miR-10a-5p* (guide strand) and *miR-10a-3p* (passenger strand), are derived from pre-*miR-10a*.

Table 1. Characteristics of primary ccRCC clinical specimens

No.	Age (years)	Sex	Pathology	Grade	pT	INF	v	ly	e.g or ig	fc	im	rc	rp	s
1	71	F	Clear cell	G2	T1a	a	0	0	e.g	1	0	0	0	0
2	74	M	Clear cell	G1>G2	T1a	a	0	0	e.g	1	0	0	0	0
3	59	M	Clear cell	G3>G2	T1b	a	0	0	e.g	1	0	0	0	0
4	79	M	Clear cell	G2>G3>G1	T1a	a	0	0	e.g	1	0	0	0	0
5	52	M	Clear cell	G2>G3	T1b	a	0	0	e.g	1	1	0	0	0
6	64	M	Clear cell	G2>G3>G1	T3a	b	1	0	ig	0	1	1	0	0
7	67	M	Clear cell	G2>G3>G1	T3a	b	1	0	ig	1	0	0	0	0
8	59	M	Clear cell	G3	T3a	b	1	0	ig	0	0	0	0	0
9	73	M	Clear cell	G1>>G3	T2a	a	0	1	e.g	1	0	0	0	0
10	77	M	Clear cell	G1>G2	T1b	a	0	0	e.g	1	0	0	0	0
11	51	F	Clear cell	G2>G1>G3	T3a	b	1	0	ig	0	0	0	0	0
12	84	F	Clear cell	G2	T1a	a	0	0	e.g	0	0	0	0	0
13	78	M	Clear cell	G2>G1≫G3	T1b	b	0	0	e.g	1	0	0	0	0
14	44	M	Clear cell	G2>G1	T1a	b	0	0	e.g	1	0	0	0	0
15	57	M	Clear cell	G2	T1b	a	0	0	e.g	0	0	0	0	0

ccRCC, clear cell renal cell carcinoma; e.g, expansive growth; fc, capsular formation; ig, infiltrative growth; im, intrarenal metastasis; INF, infiltration; ly, lymph node; rc, renal capsule invasion; rp, pelvis invasion; s, sinus invasion; v, vein.

Table 2. Characteristics of ccRCC autopsy specimens after TKI treatment

Patient	Specimen no.	Location	Age (years)	Stage at diagnosis				Histological type	Grade	Treatment	Treatment duration (months)	Pathological feature of autopsy	Survival from diagnosis (months)
				Stage	cT	cN	cM						
A	1	Kidney	69	IV	4	2	1	Clear cell carcinoma	3	Sunitinib Temsirolimus	8.5	Multiple lung metastasis Bone metastasis	9.1
	2	Lymph node											
	3	Liver											
	4	Tumor emboli											
B	5	Kidney	80	III	3c	0	0	Clear cell carcinoma	3	Sunitinib	0.7	IVC tumor emboli	1.8
	6	Tumor emboli											
C	7	Mesenterium	62	I	1b	0	0	Clear cell carcinoma with spindle cell carcinoma	3	Sunitinib Axitinib	34	Multiple bone metastasis Pleural metastasis Lung metastasis Para-aorta lymph node metastasis	43
	8	Lymph node											
	9	Pleura											
D	10	Kidney	69	IV	X	2	1	Clear cell carcinoma	3	Pazopanib	2	Multiple lung metastasis Multiple bone metastasis Kidney metastasis Adrenal metastasis Pleural metastasis Skin metastasis	5.1
	11	Lymph node											
	12	Lymph node											
	13	Adrenal gland											
	14	Skin											
	15	Pleura											

ccRCC, clear cell renal cell carcinoma; TKI, tyrosine kinase inhibitor.

Analysis of our original miRNA expression signature of TKI failure in patients with RCC showed that antitumor *miR-101* directly regulated ubiquitin-like with PHD and ring finger domains 1 (*UHRF1*), which acted as an oncogene in RCC cells.[22] Based on this signature, we focused on *miR-10a-5p* because *miR-10a-5p* is significantly downregulated in TKI-treated ccRCC compared with primary ccRCC.[22] Moreover, The Cancer Genome Atlas[23] database showed that the overall survival of patients in the low *miR-10a-5p* expression group was significantly shorter than that of patients in the high expression group in ccRCC ($P = 0.00991$, Fig. 1a).

The aims of the present study were to investigate the functional significance of *miR-10a-5p* and to identify the molecular targets regulated by *miR-10a-5p* in ccRCC cells. Our data showed that restoration of mature *miR-10a-5p* inhibited ccRCC cell proliferation, migration, and invasion. Furthermore, our data demonstrated that the *SKA1* gene was overexpressed in primary RCC and advanced RCC specimens and was directly regulated by *miR-10a-5p* in RCC cells. These results demonstrated that *SKA1* was involved in RCC pathogenesis, implying that *SKA1* could be a novel diagnostic and therapeutic target for patients with advanced RCC.

Materials and Methods

ccRCC clinical specimens and cell culture. A total of 15 pairs of ccRCC specimens and adjacent noncancerous specimens were collected from patients who had undergone radical nephrectomy at Chiba University Hospital (Chiba, Japan) from 2012 to 2015. Clinicopathological characteristics of the patients are summarized in Table 1. Four patients who died of ccRCC after TKI treatment underwent autopsy at Teikyo University Chiba Medical Center Hospital from 2012 to 2016, as summarized in Table 2. These specimens were staged according to the General Rule for Clinical and Pathological Studies on Renal Cell Carcinoma based on the American Joint Committee on Cancer (AJCC)-UICC TNM classification.[24] Written consent for tissue donation for research purposes was obtained from each patient before tissue collection. We used two human ccRCC cell lines (786-O and A498) obtained from the American Type Culture Collection (ATCC, Manassas, VA, USA) as previously described.[22,25–28]

RNA extraction. Total RNA was extracted using TRIzol reagent (Invitrogen, Carlsbad, CA, USA) according to the manufacturer's protocol, as described previously.[22,25–28] RNA quality was confirmed using an Agilent 2100 Bioanalyzer (Agilent Technologies, Santa Clara, CA, USA).

Quantitative real-time reverse transcription polymerase chain reaction (qRT-PCR). The procedure for PCR quantification was described previously.[22,25–28] Expression levels of *miR-10a-5p* (Assay ID: 000387) were analyzed by TaqMan qRT-PCR (TaqMan MicroRNA Assay; Applied Biosystems, Foster City, CA, USA) and normalized to the expression of *RNU48* (assay ID: 001006; Applied Biosystems). TaqMan probes and primers for *SKA1* (P/N: Hs00536843_m1; Applied Biosystems), *GAPDH* (internal control; P/N: Hs02758991_m1; Applied Biosystems), and *GUSB* (internal control; P/N: Hs00939627_ml; Applied Biosystems) were assay-on-demand gene expression products.

Transfections with mature miRNA, siRNA, or plasmid vectors. The following mature miRNA species were used in this study: mature miRNA and Pre-miR miRNA Precursor (*hsa-miR-10a-5p*; P/N: AM17100; Applied Biosystems). The following siRNAs were used: Stealth Select RNAi siRNA, si-*SKA1*

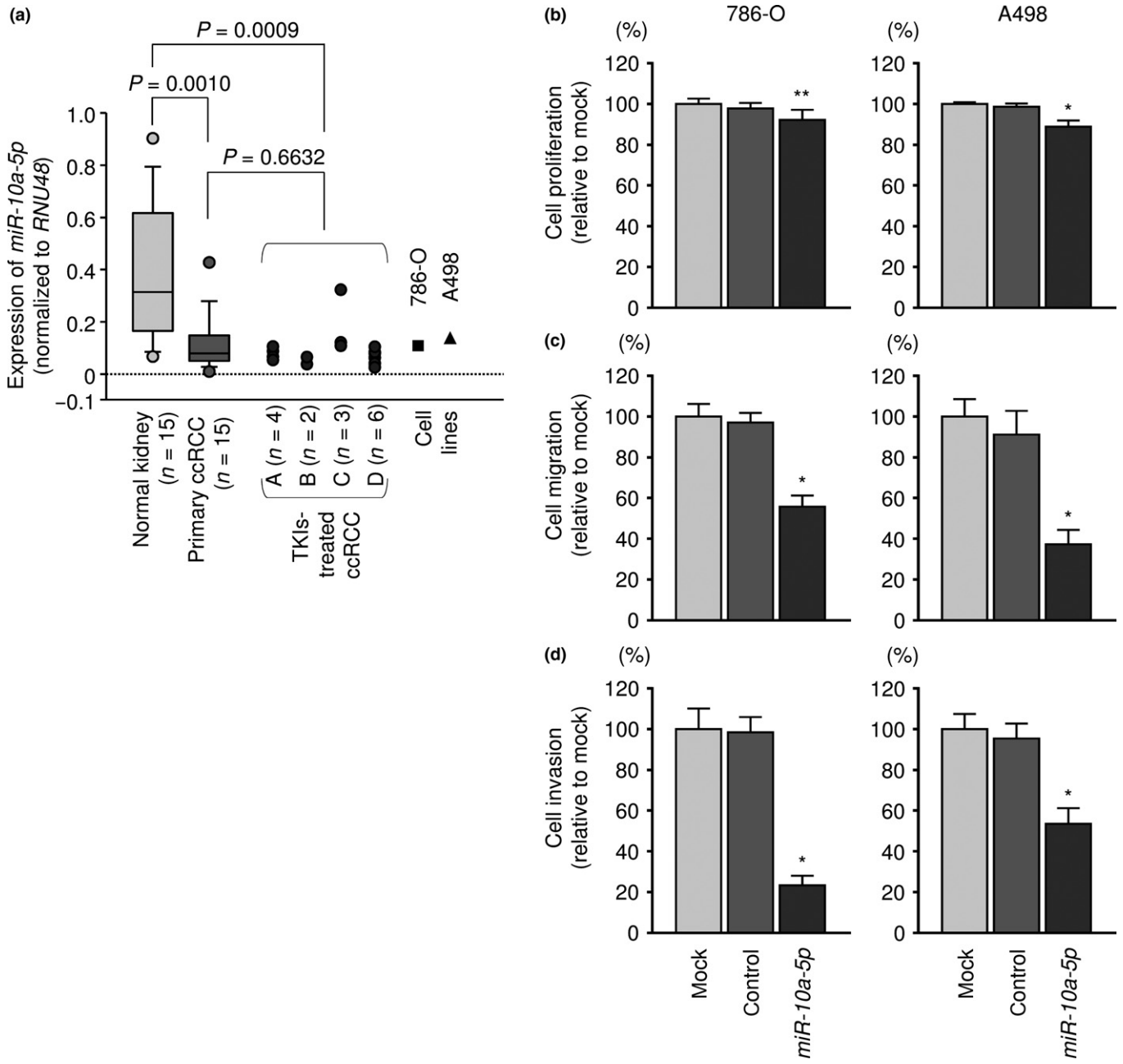

Fig. 2. Expression levels of *miR-10a-5p* in clear cell renal cell carcinoma (ccRCC) clinical specimens and functional significance of *miR-10a-5p* in ccRCC cells. (a) Expression levels of *miR-10a-5p* in ccRCC clinical specimens and cell lines determined using qRT-PCR. *RNU48* was used as an internal control. TKI, tyrosine kinase inhibitor. (b) Cell proliferation was determined by XTT assays 72 h after transfection with 10 nM *miR-10a-5p*. $*P < 0.0001$, $**P < 0.01$. (c) Cell migration activity was assessed by wound-healing assays 48 h after transfection with 10 nM *miR-10a-5p*. $*P < 0.0001$. (d) Cell invasion activity was characterized by invasion assays 48 h after transfection with 10 nM *miR-10a-5p*. $*P < 0.0001$.

(cat. nos. HSS137392 and HSS137393; Invitrogen), and negative control miRNA/siRNA (P/N: AM17111; Applied Biosystems). *SKA1* plasmid vectors were designed and provided by ORIGENE (cat. no. RC202370; Rockville, MD, USA). miRNAs and siRNAs were incubated with Opti-MEM (Invitrogen) and Lipofectamine RNAiMax transfection reagent (Invitrogen), as previously described.[22,25–28] Plasmid vectors were incubated with Opti-MEM and Lipofectamine 3000 reagent (Invitrogen) by forward transfection following the manufacturer's protocol.

Cell proliferation, migration, and invasion assays. 786-O and A498 cells were transfected with 10 nM miRNAs or siRNAs by reverse transfection. Cell proliferation was determined by XTT assays using a Cell Proliferation Kit II (Sigma-Aldrich, St Louis, MO, USA). Cell migration was evaluated with wound healing assays. Cell invasion was analyzed using modified Boyden chambers containing Transwell-precoated Matrigel membrane filter inserts (cat. no. 354480; BD Biosciences, Bedford, MA, USA). These assays were carried out as described previously.[22,25–28] All experiments were carried out in triplicate.

Selection of putative target genes regulated by *miR-10a-5p* in ccRCC cells. To identify *miR-10a-5p* target genes, we used *in*

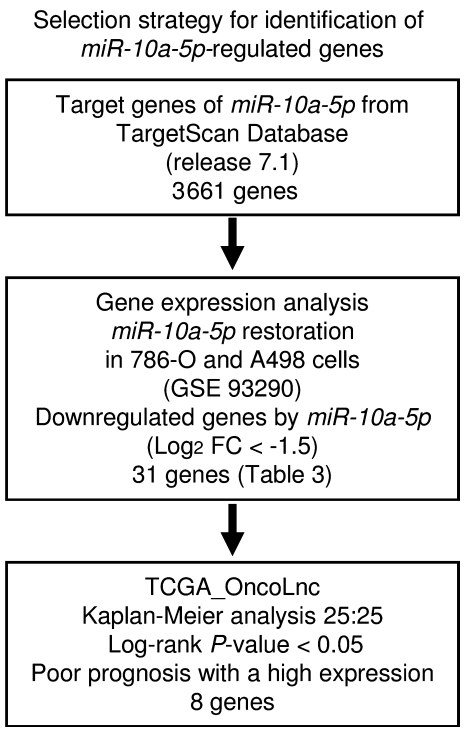

Fig. 3. Identification of *miR-10a-5p* target genes. Flow chart of the strategy for identification of *miR-10a-5p* target genes.

silico analyses and genome-wide gene expression analyses, as described previously. We used the TargetScanHuman 7.1 (June, 2016 release, http://www.targetscan.org/vert_71) database, TCGA, and OncoLnc (http://www.oncolnc.org/) to select and narrow down putative miRNA target genes.[29,30] An oligo microarray (Human Ge 60K; Agilent Technologies) was used for gene expression analysis. The microarray data were deposited into the GEO database (https://www.ncbi.nlm.nih.gov/geo/ ; accession number: GSE93290).

Western blotting. Cells were harvested 48 h after transfection, and lysates were prepared. Immunoblotting was carried out with rabbit anti-SKA1 antibodies (1:1,000 dilution, SAB2701430; Sigma-Aldrich), anti-AKT antibody (1:1000, #4691; Cell Signaling Technology, Danvers, MA, USA), anti-p-AKT antibody (1:1000, #4060; Cell Signaling Technology), anti-ERK1/2 antibody (1:1000, #4695; Cell Signaling Technology), anti-p-ERK1/2 antibody (1:2000, #4370; Cell Signaling Technology), anti-FAK antibody (1:1000, #3285; Cell Signaling Technology) and anti-p-FAK antibody (1:1000, #8556; Cell Signaling Technology), anti-SRC antibody (1:1000, #2123; Cell Signaling Technology) and anti-p-SRC antibody (1:1000, #6943; Cell Signaling Technology). Anti-glyceraldehyde 3-phosphate dehydrogenase (GAPDH) antibodies (1:10000, ab8245; Abcam, Cambridge, UK) were used as an internal loading control. Experimental procedures were carried out as described previously.[22,25–28] Protein expression was quantified by using NIH-ImageJ.

Plasmid construction and dual-luciferase reporter assays. The partial wild-type sequence of the *SKA1* 3′-UTR or that with deletion of the *miR-10a-5p* target site was inserted between the *Xho*I-*Pme*I restriction sites in the 3′-UTR of the *hRluc* gene in the psiCHECK-2 vector (C8021; Promega, Madison, WI, USA). The procedures were described previously.[22,25–28]

Immunohistochemistry. Tissue specimens were incubated overnight at 4°C with anti-SKA1 antibodies (1:500 dilution, SAB2701430; Sigma-Aldrich). The slides were treated with biotinylated goat antibodies (Histofine SAB-PO kit; Nichirei, Tokyo, Japan). The procedures were described previously.[22,25–28]

TCGA database analysis of ccRCC. To explore the clinical significance of miRNAs and target genes, we used the TCGA database. Gene expression and clinical data were retrieved from cBioportal (http://www.cbioportal.org/)[31] and OncoLnc (data downloaded on April 30, 2017). We selected high and low target genes expression groups defined by the median value, and data were analyzed by Kaplan-Meier survival curves and log-rank statistics.

Statistical analysis. Relationships between two groups and the numerical values obtained by qRT-PCR were analyzed using Mann-Whitney *U*-tests and paired *t*-tests. Spearman's rank test was used to evaluate the correlation between the expression levels of *miR-10a-5p* and *SKA1*. Relationships among more than three variables and numerical values were analyzed using Bonferroni-adjusted Mann-Whitney *U*-tests. Survival analysis was carried out using the Kaplan–Meier method and log-rank tests with JMP software (version 13; SAS Institute Inc., Cary, NC, USA); all other analyses were carried out using Expert StatView (version 5; SAS Institute Inc.).

Results

Expression levels of *miR-10a-5p* in ccRCC specimens and cell lines. The public miRNA database (miRbase: release 21) showed that *miR-10a-5p* was located on chromosome 17q21.32. The mature sequence of *miR-10a-5p* was found to be 5′-UACCCUGUAGAUCCGAAUUUGUG-3′ (Fig. 1b). We evaluated the expression of *miR-10a-5p* in clinical kidney specimens (noncancerous tissues, ccRCC tissues, and autopsy specimens of ccRCC) and cell lines. Expression levels of *miR-10a-5p* were significantly downregulated in primary cancer tissues and TKI-treated tissues compared with those in noncancerous tissues ($P = 0.0010$, $P = 0.0009$, respectively; Fig. 2a). In 786-O and A498 cells, expression levels of *miR-10a-5p* were relatively low compared with those of clinical specimens (Fig. 2a).

Effects of restoring *miR-10a-5p* on cell proliferation, migration, and invasion activities in ccRCC cell lines. To investigate the functional efficacy of *miR-10a-5p*, we carried out gain-of-function studies using miRNA transfection into 786-O and A498 cells. XTT assays showed that cell proliferation was significantly inhibited in *miR-10a-5p* transfectants compared with that in mock or miR-control transfectants (Figs 2b; S1a). Migration assays showed that cell migration activity was significantly inhibited in *miR-10a-5p* transfectants in comparison with those in mock or miR-control transfectants (Figs 2c; S2a). Similarly, Matrigel invasion assays showed that cell invasion activity was significantly inhibited in *miR-10a-5p* transfectants in comparison with those in mock or miR-control transfectants (Figs 2d; S2b).

Identification of candidate genes regulated by *miR-10a-5p* in ccRCC cells. To further elucidate the molecular mechanisms and pathways regulated by antitumor *miR-10a-5p* in ccRCC cells, we carried out a combination of *in silico* analyses and oligo microarray analyses using *miR-10a-5p* transfectants. The strategy for selection of *miR-10a-5p* target genes is shown in Figure 3. First, we used TargetScanHuman 7.1 database and identified that 3661 genes had putative target sites for *miR-10a-5p* in their 3′-UTR. Next, we paired down the 3661 genes

Table 3. Candidate target genes regulated by miR-10a-5p in clear cell renal cell carcinoma (ccRCC)

Gene Symbol	Gene name	Location	No. conserved sites	No. poorly conserved sites	Log_2 ratio (A498)	Log_2 ratio (786-O)	Log_2 ratio (average)	TCGA-KIRC OncoLnc 25:25 *P*-value
SKA1	Spindle and kinetochore-associated protein 1	18q21.1	0	1	−5.06	−2.01	−3.54	*2.72E−08
SLC7A1	Solute carrier family 7 (cationic amino acid transporter, y+ system), member 1	13q12.3	0	1	−3.38	−2.23	−2.81	2.62E−01
SUMF1	Sulfatase modifying factor 1	3p26.1	0	1	−2.35	−2.65	−2.50	9.42E−01
P4HB	Prolyl 4-hydroxylase, beta polypeptide	17q25.3	0	1	−2.61	−2.35	−2.48	*2.75E−04
USP46	Ubiquitin specific peptidase 46	4q12	1	1	−1.96	−2.9	−2.43	6.62E−02
ELOVL2	ELOVL fatty acid elongase 2	6p24.2	1	0	−2.25	−2.39	−2.32	*6.39E−04
KCTD13	Potassium channel tetramerization domain containing 13	16p11.2	0	1	−2.69	−1.72	−2.21	*4.00E−06
LINC00908	Long intergenic non-protein coding RNA 908	18q23	0	1	−2.62	−1.79	−2.21	1.52E−01
SUN2	Sad1 and UNC84 domain containing 2	22q13.1	0	3	−2.10	−2.31	−2.21	1.31E−01
FCF1	FCF1 rRNA-processing protein	14q24.3	0	1	−2.51	−1.84	−2.18	8.74E−04
ARG2	Arginase 2	14q24.1	0	1	−2.06	−2.25	−2.16	6.91E−01
SLAMF7	SLAM family member 7	1q23.3	0	1	−1.52	−2.77	−2.15	1.23E−01
PRKAA2	Protein kinase, AMP-activated, alpha 2 catalytic subunit	1p32.2	1	3	−1.66	−2.58	−2.12	2.10E−09
FANCC	Fanconi anemia, complementation group C	9q22.32	0	3	−2.23	−2.00	−2.12	4.29E−03
PDCL	Phosducin-like	9q33.2	0	1	−2.03	−2.03	−2.03	1.19E−03
PSIP1	PC4 and SFRS1 interacting protein 1	9p22.3	0	1	−2.51	−1.53	−2.02	4.96E−02
CD3D	CD3d molecule, delta (CD3-TCR complex)	11q23.3	0	2	−2.20	−1.82	−2.01	9.89E−02
C1QL4	Complement component 1, q subcomponent-like 4	12q13.12	0	1	−1.97	−2.04	−2.01	7.02E−03
SDC1	syndecan 1	2p24.1	1	0	−1.94	−2.05	−2.00	6.76E−01
DNAL4	Dynein, axonemal, light chain 4	22q13.1	0	1	−1.91	−2.06	−1.99	7.34E−01
NUP62CL	Nucleoporin 62kDa C-terminal like	Xq22.3	0	2	−1.7	−2.03	−1.87	4.12E−02
MTUS1	Microtubule associated tumor suppressor 1	8p22	0	1	−1.93	−1.76	−1.85	4.03E−03
RTN4R	Reticulon 4 receptor	22q11.21	0	1	−2.07	−1.6	−1.84	*1.24E−05
PM20D2	Peptidase M20 domain containing 2	6q15	0	1	−2.04	−1.56	−1.80	2.92E−02
PCBD1	Pterin-4 alpha-carbinolamine dehydratase/dimerization cofactor of hepatocyte nuclear factor 1 alpha	10q22.1	0	1	−1.55	−2.03	−1.79	4.00E−01
APAF1	Apoptotic peptidase activating factor 1	12q23.1	0	3	−1.90	−1.63	−1.77	*1.18E−03
DOHH	Deoxyhypusine hydroxylase/ monooxygenase	19p13.3	0	2	−1.78	−1.56	−1.67	*6.16E−03
AIM1	Absent in melanoma 1	6q21	0	1	−1.71	−1.55	−1.63	2.67E−01
ANXA7	Annexin A7	10q22.2	1	0	−1.50	−1.65	−1.58	5.17E−02
HS3ST1	Heparan sulfate (glucosamine) 3-O-sulfotransferase 1	4p15.33	0	1	−1.54	−1.56	−1.55	2.99E−03
IMPAD1	Inositol monophosphatase domain containing 1	8q12.1	0	1	−1.52	−1.56	−1.54	*5.59E−03

*Kaplan–Meier survival analysis $P < 0.05$. Poor prognosis with high expression in ccRCC.

based on gene expression data (GEO database accession number: GSE93290), and 31 genes were markedly downregulated after transfection of 786-O and A498 cells with *miR-10a-5p* (fold-change $log_2 < -2.0$; Table 3). Finally, we checked the expression status of these 31 genes and the clinical significance of ccRCC using the OncoLnc database (http://www.oncolnc.org/). Kaplan-Meier survival curves showed that high expression of eight genes was associated with poor prognosis in ccRCC (Table 3; Figs 4a, 5). Among these genes, we focused on *SKA1*, which was most downregulated by transfection of *miR-10a-5p*, and showed the most dramatic difference in OncoLnc prognostic analysis ($P = 2.72E-08$, Fig. 4a).

Expression of SKA1 in ccRCC clinical specimens. A total of 15 pairs of primary ccRCC specimens, adjacent noncancerous specimens, and TKI-treatment failure autopsy specimens from 15 sites were used for the expression analysis of *SKA1* by qRT-PCR. Expression of *SKA1* was significantly upregulated in primary cancer tissues compared with that in normal tissues ($P = 0.0011$; Fig. 4b) and was significantly higher in autopsy specimens than in primary cancer tissues ($P = 0.0011$; Fig. 4b). Additionally, Spearman's rank test indicated a negative correlation between the expression levels of *miR-10a-5p* and *SKA1* (Fig. 4c).

Furthermore, to analyze SKA1 protein expression, immunohistochemistry was carried out with a ccRCC tissue

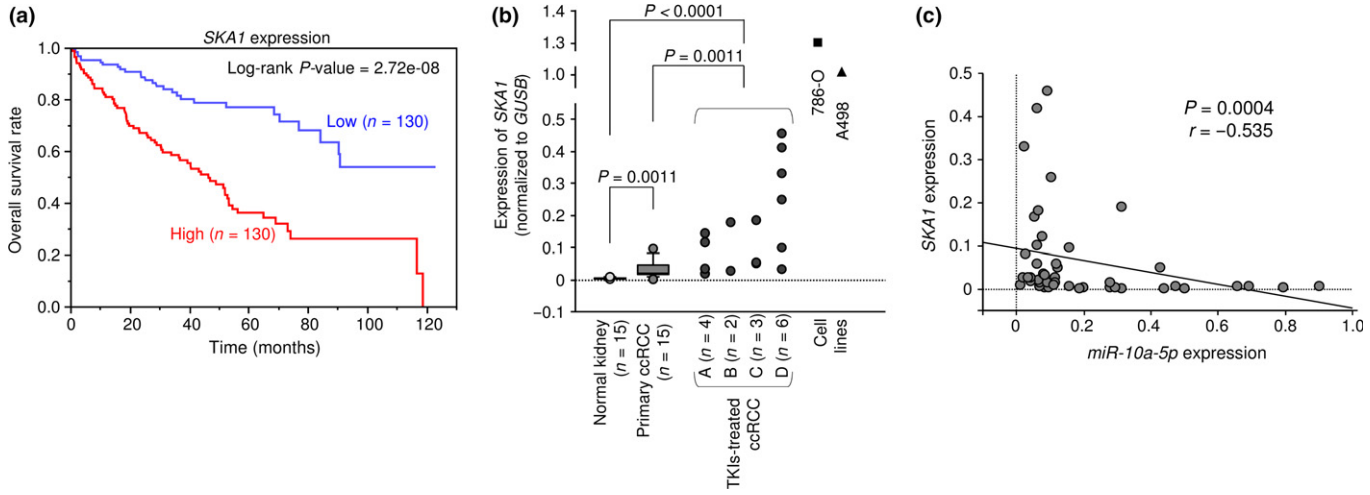

Fig. 4. Kaplan-Meier survival curves based on *SKA1* expression in patients with clear cell renal cell carcinoma (ccRCC), and expression levels of *SKA1* in ccRCC clinical specimens. (a) Kaplan-Meier survival curve for overall survival rate based on *SKA1* expression in patients with ccRCC. (b) Expression levels of *SKA1* in ccRCC clinical specimens and cell lines. *GUSB* was used as an internal control. TKI, tyrosine kinase inhibitor. (c) Negative correlation between *miR-10a-5p* and *SKA1*.

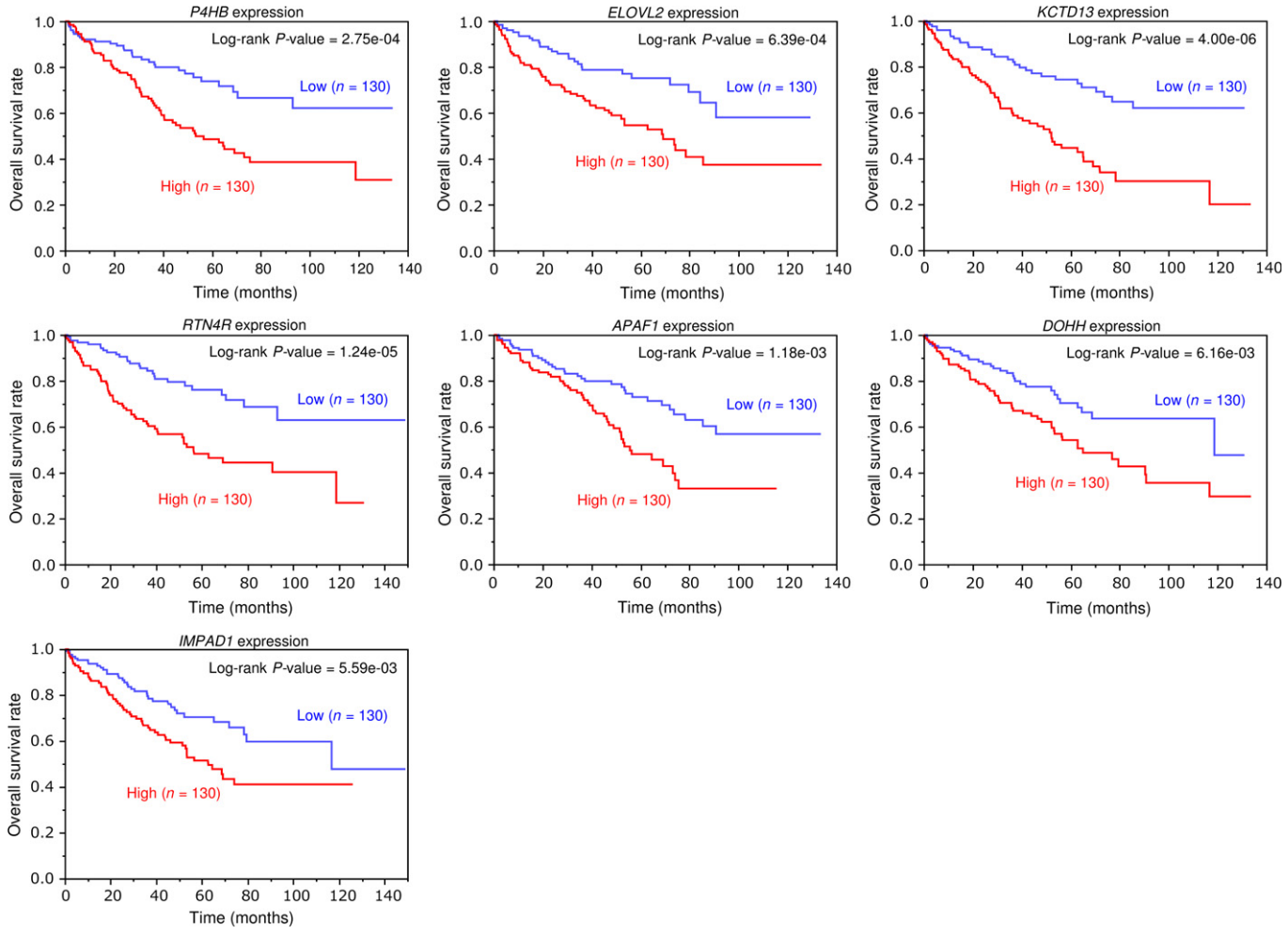

Fig. 5. Kaplan-Meier survival curves for overall survival rates based on expression of seven genes, excluding *SKA1*, in patients with clear cell renal cell carcinoma (ccRCC).

microarray (cat. no. KD806; US Biomax, Rockville, MD, USA) and autopsy specimens after TKI treatment (Patient D, Table 2). Patient characteristics for samples used in the tissue microarray are as described in http://www.biomax.us/tissue-arrays/Kidney/KD806. SKA1 was strongly expressed in primary ccRCC tissues and autopsy specimens after

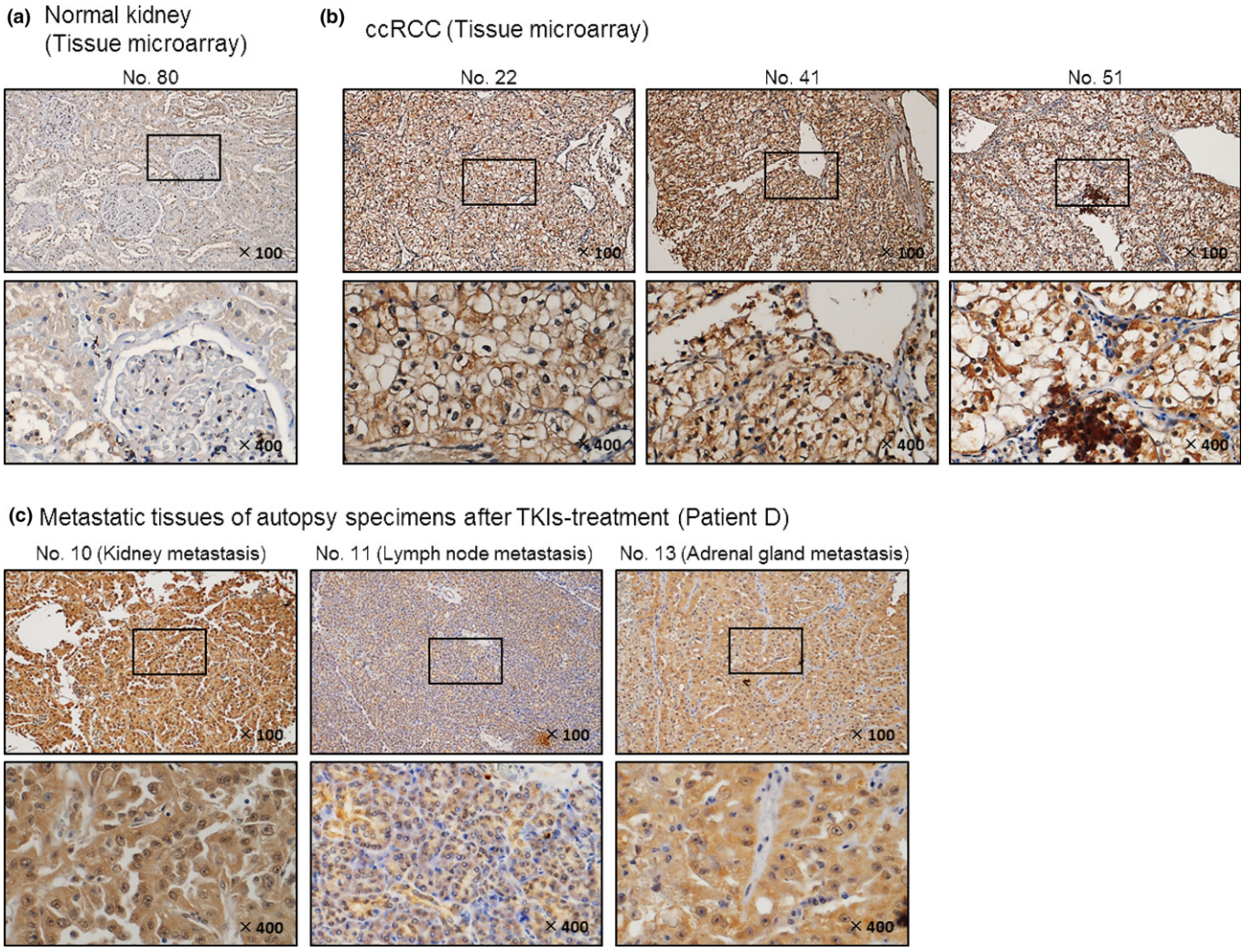

Fig. 6. Expression of SKA1 in clinical clear cell renal cell carcinoma (ccRCC) specimens using a tissue microarray and autopsy tissues. Representative immunohistochemical staining for SKA1 in a ccRCC tissue microarray (cat. no. KD806; US Biomax, Inc., Rockville, MD, USA) and autopsy specimens after tyrosine kinase inhibitor (TKI) treatment (Patient D, Table 2). SKA1 was strongly expressed in ccRCC tissues. (a) Normal kidney. (b) ccRCC tissues. (c) ccRCC autopsy tissues after TKI treatment.

TKI treatment compared with that in normal kidney (Fig. 6).

***SKA1* was directly regulated by *miR-10a-5p* transfection in ccRCC cells.** We carried out qRT-PCR and western blotting to validate whether restoration of *miR-10a-5p* in 786-O and A498 cells reduced the expression of SKA1. Expression of *SKA1* mRNA was significantly suppressed by *miR-10a-5p* transfection compared with that in mock- or miR-control-transfected cells (Fig. 7a). Similarly, SKA1 protein expression was repressed in the *miR-10a-5p* transfectants (Fig. 7b).

Next, we carried out luciferase reporter assays to determine whether *SKA1* mRNA had a functional target site. The TargetScan database predicted that *miR-10a-5p* bound at position 28–35 in the 3′-UTR of *SKA1*. We used vectors encoding a partial wild-type sequence of the 3′-UTR of *SKA1* mRNA, including the predicted *miR-10a-5p* target site, or a vector lacking the *miR-10a-5p* target site. Luminescence intensity was significantly reduced by cotransfection with *miR-10a-5p* and the vector carrying the wild-type 3′-UTR of *SKA1*. However, luminescence intensity was not suppressed when the target site of *miR-10a-5p* was deleted from the vectors (Fig. 7c).

Effects of silencing *SKA1* in ccRCC cell lines. To examine the functional significance of *SKA1*, we carried out loss-of-function studies using si-*SKA1* transfectants. First, we evaluated the knockdown efficiency of si-*SKA1* transfection in 786-O and A498 cells. In this study, we used two types of si-*SKA1* (si-*SKA1*-1 and si-*SKA1*-2). qRT-PCR and western blotting analyses showed that transfection with both siRNAs effectively downregulated *SKA1* mRNA and SKA1 protein expression in 786-O and A498 cells (Fig. 8a,b). Furthermore, functional assays indicated that si-*SKA1* transfection markedly inhibited cell proliferation, migration, and invasion in comparison with mock- or si-control-transfected cells (Figs 8c; S1b, S3a, S4a).

Effects of cotransfection of *SKA1/miR-10a-5p* in 786-O cells. To validate whether the molecular pathway of *SKA1/miR-10a-5p* was critical for the progression of ccRCC, we carried out *SKA1* rescue experiments by cotransfection with *SKA1* and *miR-10a-5p* in 786-O cells. SKA1 protein expression by Western blotting analysis is shown in Figure 9a. Functional assays showed that the migration and invasion abilities of ccRCC cells were recovered by *SKA1* and *miR-10a-5p* transfection compared with cells with restored *miR-10a-5p* only (Figs 9b–

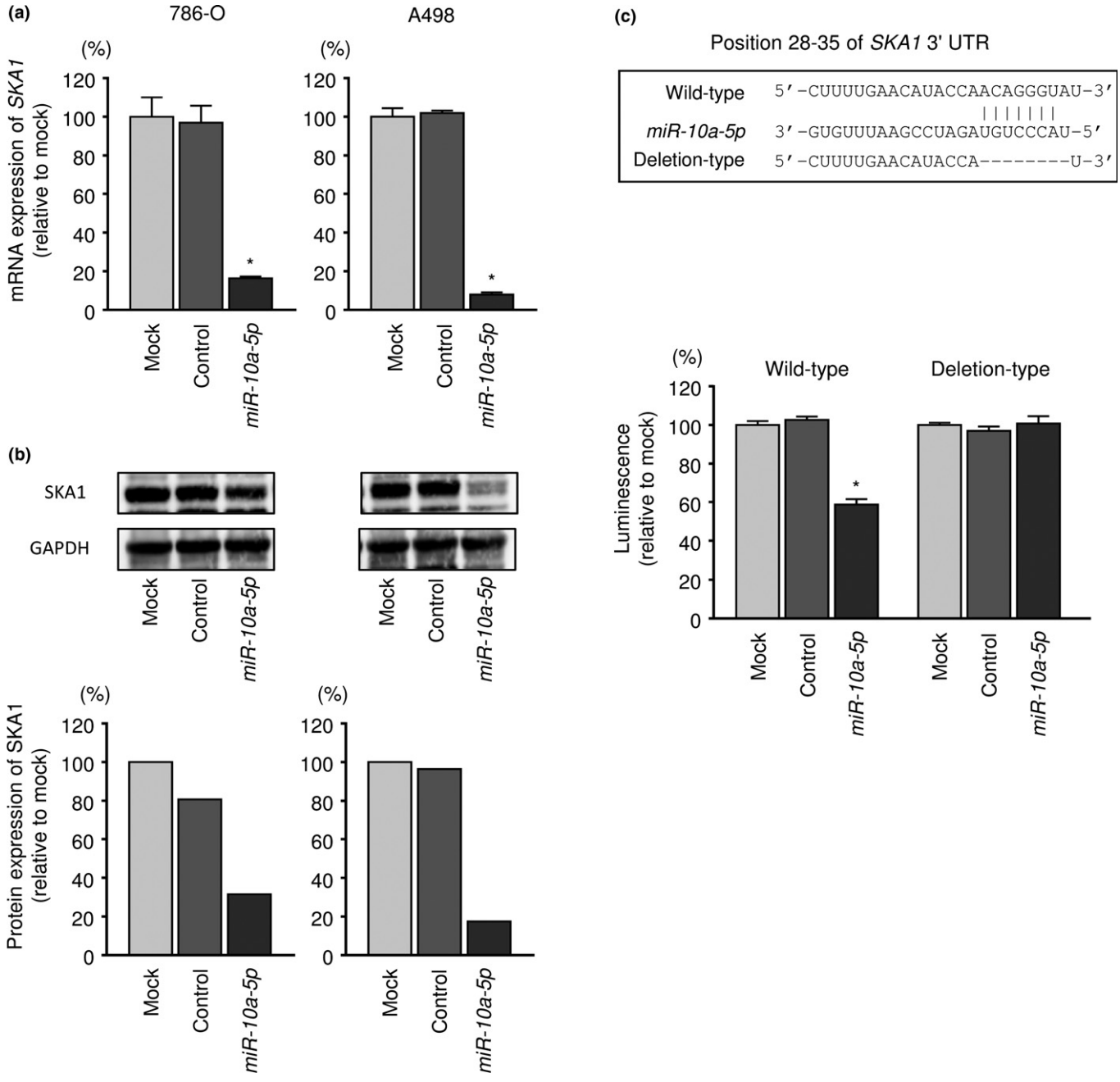

Fig. 7. Direct regulation of *SKA1* by *miR-10a-5p* in clear cell renal cell carcinoma (ccRCC) cells. (a) *SKA1* mRNA expression was evaluated using qRT-PCR in 786-O and A498 cells 48 h after transfection with *miR-10a-5p*. *GAPDH* was used as an internal control. *$P < 0.0001$. (b) SKA1 protein expression was evaluated by western blotting in 786-O and A498 cells 72 h after transfection with *miR-10a-5p*. GAPDH was used as a loading control. (c) *miR-10a-5p* binding site in the 3′-UTR of *SKA1* mRNA. Dual luciferase reporter assays in 786-O using vectors encoding the putative *miR-10a-5p* target site of *SKA1* 3′-UTR (positions 28-35). Data were normalized by expression ratios of *Renilla*/firefly luciferase activities. *$P < 0.0001$.

d; S1c, S5a,b). These results supported that *SKA1* affected the aggressiveness of ccRCC cells.

Clinical significance of *SKA1* in ccRCC. To explore the clinical significance of *SKA1* in ccRCC, we analyzed Kaplan-Meier curves of DFS rates according to the expression level of *SKA1*, and the relationships among *SKA1* expression and cancer stage, tumor stage, and histological grade in ccRCC were evaluated using the TCGA-KIRC database. Kaplan-Meier curves for DFS rates showed that the DFS of the high *SKA1* expression group was significantly shorter than that of the low expression group in ccRCC ($P < 0.0001$, Fig. 10a). Additionally, expression levels of *SKA1* were significantly increased in cases of advanced disease stage, advanced T stage, and advanced histological grade (Fig. 10b–d). These analyses suggested that *SKA1* affected disease progression and malignancy in ccRCC. Similarly, TCGA data analysis results of clinical significance for the other seven genes are shown in Figures S6–S9.

Effects of *SKA1* downstream signaling by si-*SKA1* knockdown or *miR-10a-5p* restoration in RCC cells. We investigated the

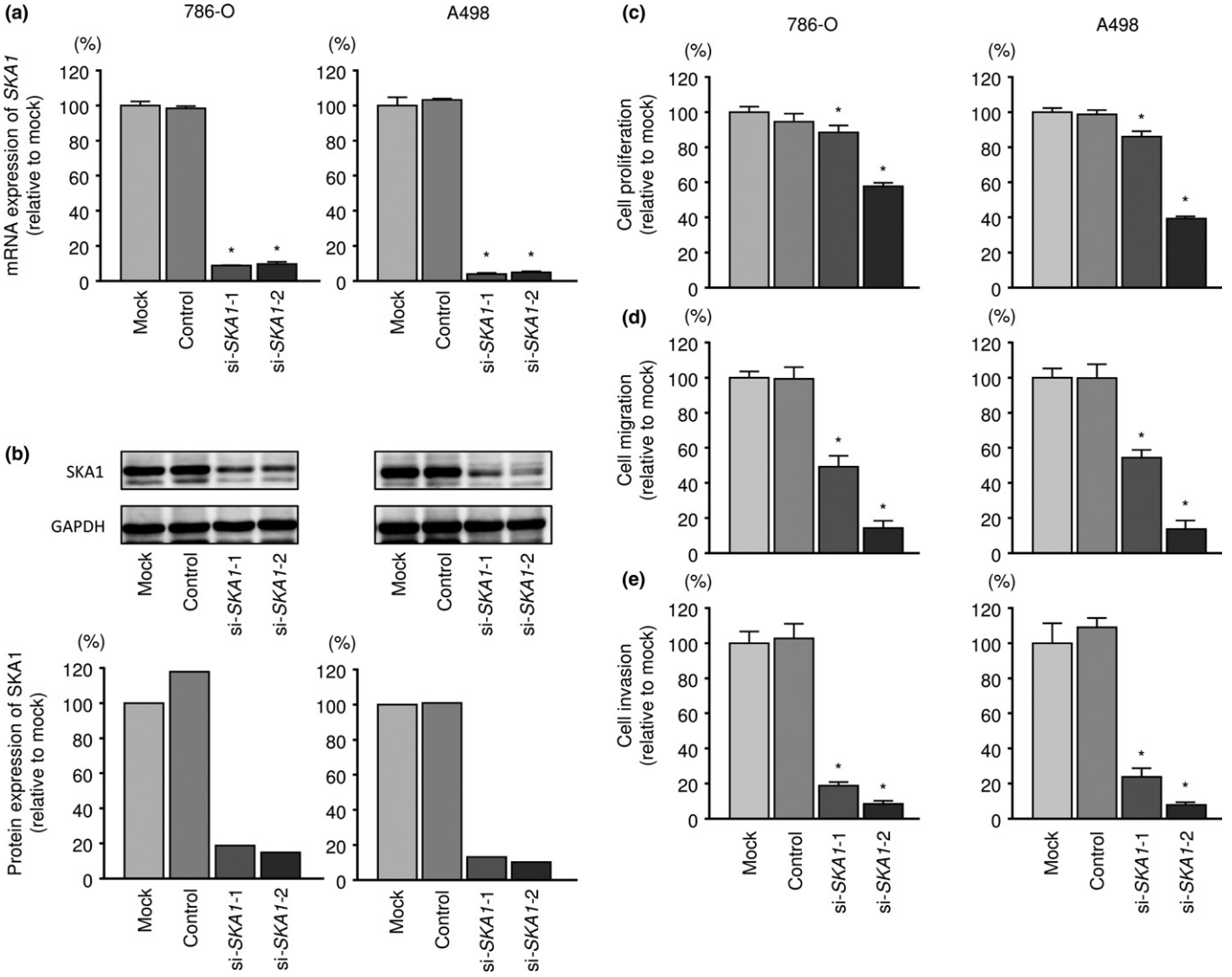

Fig. 8. Effects of *SKA1* silencing on clear cell renal cell carcinoma (ccRCC) cell lines. (a) *SKA1* mRNA expression was evaluated using qRT-PCR analysis of 786-O and A498 cells 48 h after transfection with si-*SKA1*-1 or si-*SKA1*-2. *GAPDH* was used as an internal control. *$P < 0.0001$. (b) SKA1 protein expression was evaluated by western blotting analysis of 786-O and A498 cells 72 h after transfection with *miR-10a-5p*. GAPDH was used as a loading control. (c) Cell proliferation was determined using XTT assays 72 h after transfection with 10 nM si-*SKA1*-1 or si-*SKA1*-2. *$P < 0.0001$. (d) Cell migration activity was assessed by wound-healing assays 48 h after transfection with 10 nM *si-SKA1*-1 or *si-SKA1*-2. *$P < 0.0001$. (e) Cell invasion activity was characterized by invasion assays 48 h after transfection with 10 nM *si-SKA1*-1 or *si-SKA1*-2. *$P < 0.0001$.

downstream signals of *miR-10a-5p*/*SKA1* axis in 786-O cells using mature *miR-10a-5p* or si-*SKA1* transfectants. To explore the downstream survival pathways of *miR-10a-5p*/*SKA1* axis, phosphorylation of ERK1/2 (Thr 202/Tyr 204), AKT (Ser 473), FAK (Tyr 397) and SRC (Tyr 416) was examined. Knockdown of *SKA1* or restoration of *miR-10a-5p* markedly reduced the phosphorylation of ERK1/2, AKT, FAK and SRC (Fig. 11).

Discussion

Based on the underlying molecular oncogenic mechanisms of RCC, several molecular targeted agents have been developed to improve the prognosis of patients with advanced RCC.[10,11] However, although almost all patients with RCC respond to initial treatment with molecular targeted therapies, cancer cells ultimately become resistant to these treatments.[12,32,33] Several molecular mechanisms of drug resistance have been reported in RCC; however, all of these mechanisms are not sufficient to explain the observed changes in cancer cells. Understanding these molecular mechanisms using current genomic approaches is the first step to overcoming drug resistance in RCC cells.

To investigate the molecular mechanisms of drug resistance in RCC cells, we constructed a miRNA expression signature using autopsy specimens from patients with ccRCC who exhibited TKI-treatment failure.[22] Our present data demonstrated that *miR-10a-5p* acted as an antitumor miRNA in RCC cells. TCGA database analyses indicated that downregulation of *miR-10a-5p* was associated with poor prognosis in patients with RCC. *miR-10a* belongs to the *miR-10* family together with *miR-10b*, and *miR-10a-5p* is a guide strand of *miR-10a*. Previous studies have indicated that *miR-10a* is deregulated in several types of cancers. [34–37] In different types of cancer, *miR-10a* has dual functions as either a cancer-promoting or cancer-suppressing miRNA. In RCC, a recent study showed that *miR-10a-5p* is a predictor of progression and survival for RCC;[38] however, the functional significance and relevant

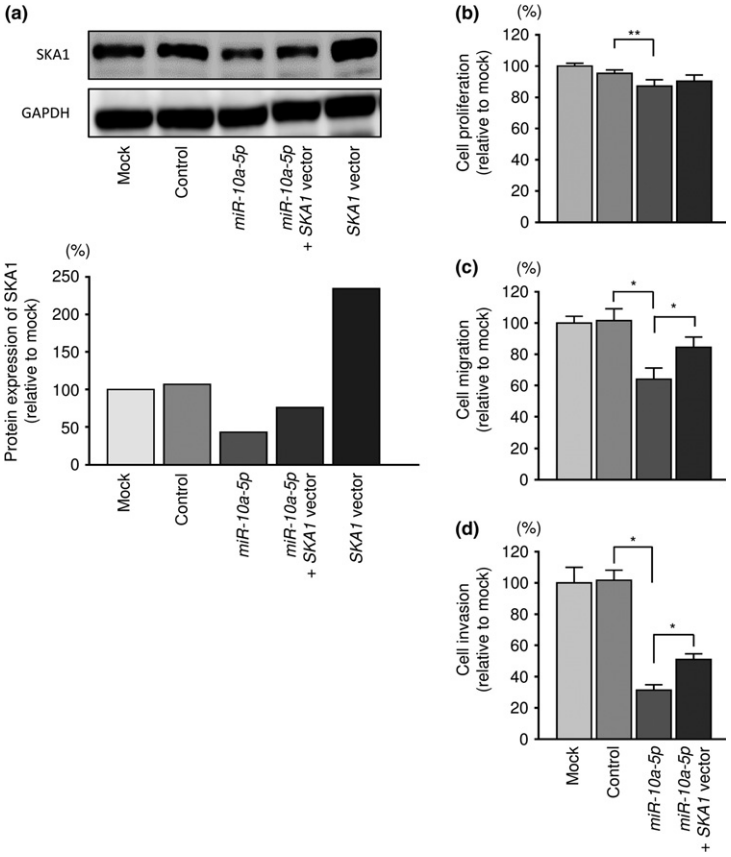

Fig. 9. Effects of cotransfection of *SKA1*/*miR-10a-5p* in 786-O cells. (a) SKA1 protein expression was evaluated by western blotting analysis of 786-O cells 72 h after reverse transfection with *miR-10a-5p* and 48 h after forward transfection with the *SKA1* vector. GAPDH was used as a loading control. (b) Cell proliferation was determined using XTT assays 72 h after reverse transfection with *miR-10a-5p* and 48 h after forward transfection with the *SKA1* vector. $^{**}P < 0.01$. (c) Cell migration activity was assessed by wound-healing assays 48 h after reverse transfection with *miR-10a-5p* and 24 h after forward transfection with the *SKA1* vector. $^{*}P < 0.0001$. (d) Cell invasion activity was characterized by invasion assays 48 h after reverse transfection with *miR-10a-5p* and 48 h after forward transfection with *SKA1* vector. $^{*}P < 0.0001$.

molecular mechanisms of *miR-10a-5p* in cancer progression are still unknown.

One of the main challenges in miRNA studies is identification of miRNA-target genes and RNA networks mediated by antitumor miRNAs in cancer cells. A total of 31 genes were identified as putative targets of *miR-10a-5p* regulation in ccRCC cells in this study. Among them, eight genes (*SKA1*, *P4HB*, *ELOVL2*, *KCTD13*, *RTN4R*, *APAF1*, *ANXA7*, and *IMPAD1*) were associated with poor prognosis in patients with RCC by TCGA analyses. We focused on the *SKA1* gene because overexpression of this gene showed the most significant association with poor prognosis in RCC. Another seven genes may also be involved in the pathology of RCC. Analyses of these genes are important for elucidating the molecular mechanisms of RCC oncogenesis, metastasis and drug resistance.

It is well known that one mRNA was regulated by a number of miRNAs. TargetScan database searching showed that *SKA1* was a putative target for *miR-10b-5p*, *miR-24-3p* and *miR-23b-3p* which were significantly downregulated in our miRNA signature of TKI treatment of RCC specimens.[22] Our previous studies demonstrated that *miR-24-3p* and *miR-23b-3p* acted as antitumor miRNAs targeting several oncogenic genes.[39,40] Also, *miR-10b-5p* functioned as an antitumor miRNA in several types of cancers including RCC.[41–43] We made the following hypothesis from these findings, *SKA1* is regulated by several antitumor miRNAs which contribute to RCC pathogenesis and drug resistance. From the analyses of these miRNAs, it can be expected to lead to elucidation of the mechanism of drug resistance of RCC.

Several studies have indicated that *SKA1* is involved in the growth and proliferation of various types of cancer, including oral adenosquamous and hepatocellular carcinoma, bladder cancer, gastric cancer, prostate cancer, thyroid cancer, non-small cell lung cancer, and glioblastoma.[44–51] In the human genome, *SKA1*, *SKA2*, and *SKA3* form the SKA complex. During mitosis, the SKA complex is localized between the outer kinetochore interface and the spindle microtubules. This complex is indispensable for stabilizing adhesion of spindle microtubules to kinetochores and maintaining the metaphase plate; therefore, this complex is critical for appropriate chromosome segregation during mitosis.[52–54] Interestingly, the expression of *SKA1* contributes to cisplatin resistance in lung cancer cells by protecting the cells from cisplatin-induced apoptosis.[50] Knockdown of *SKA1* decreases the activation of extracellular signal-regulated kinase (ERK1/2) and AKT-mediated signaling pathways in lung cancer cells.[50] Another study also demonstrated that knockdown of *SKA1* alleviated the activation of ERK1/2 and AKT in bladder cancer cells.[46] In adenoid cystic carcinoma, knockdown of *SKA1* inhibited cell proliferation, invasion, and migration, and cell cycle arrest by regulating cell cycle-promoting genes and the matrix metalloproteinase-9 gene.[55] These findings suggested that the expression of *SKA1* may be induced by cancer-promoting genes and could contribute to cancer cell aggressiveness and drug resistance. Many reports have demonstrated that acquired resistance of RCC cells to molecular targeted therapies induces cancer-promoting genes and activates several alternative pathways.[12,56,57] A previous study showed that sunitinib treatment significantly suppressed phosphorylation of ERK1/2 and AKT in TKI-sensitive RCC cells, whereas inhibition of phosphorylation was not observed in TKI-resistant RCC cells.[58] In this study, phosphorylation of ERK1/2 and AKT was suppressed by knockdown of *SKA1* and restoration of *miR-10a-5p*. This suggests that downregulation of *miR-10a-5p* and overexpression of the *SKA1* axis may be involved in resistance to VEGF- and mTOR-targeted treatments in RCC.

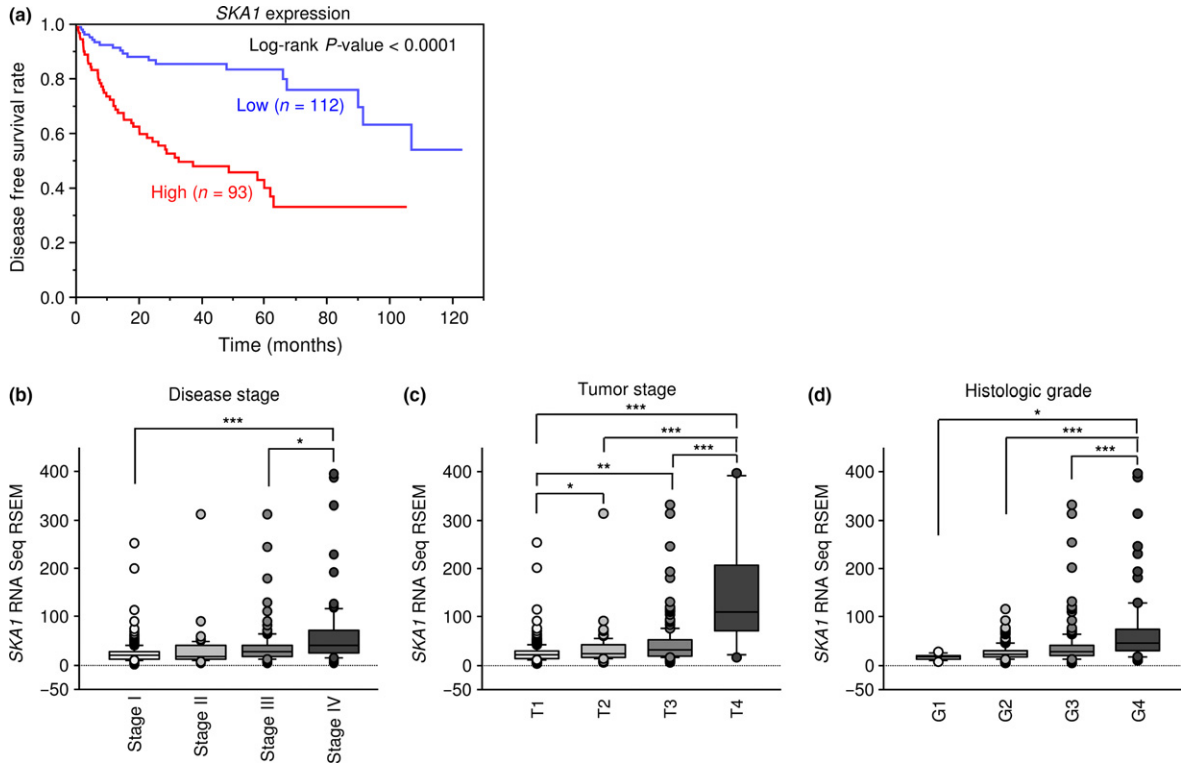

Fig. 10. Kaplan-Meier survival curve based on *SKA1* expression in patients with clear cell renal cell carcinoma (ccRCC), and expression levels of *SKA1* according to TNM stage, T stage, and histological grade. (a) Kaplan-Meier survival curves for disease-free survival rate based on *SKA1* expression in patients with ccRCC. (b-d) Expression levels of *SKA1* were significantly increased in cases of advanced TNM stage, advanced T stage, and advanced histological grade. $*P < 0.01$, $**P < 0.001$, $***P < 0.0001$.

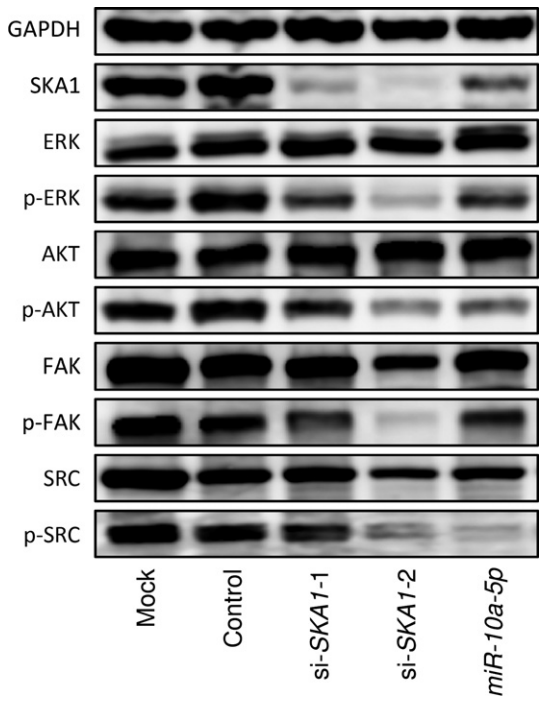

Fig. 11. Effects of the gene encoding SKA1 protein on downstream signaling. Knockdown of *SKA1* and restoration of *miR-10a-5p* in 786-O cells reduced the phosphorylation of ERK1/2, AKT, FAK and SRC. GAPDH was used as a loading control.

In conclusion, downregulation of *miR-10a-5p* was detected in the miRNA signature of TKI-failure RCC and acted as an antitumor miRNA in RCC cells. To the best of our knowledge, this is the first study showing that antitumor *miR-10a-5p* directly regulated *SKA1* in RCC cells. Overexpression of SKA1 was observed in primary and TKI-failure RCC specimens. Moreover, downregulation of *miR-10a-5p* and overexpression of *SKA1* were associated with poor prognosis in patients with RCC. Elucidation of *miR-10a-5p/SKA1*-mediated molecular networks may improve our understanding of the pathogenesis of primary RCC and molecular targeted treatment failure in RCC and facilitate the development of new treatment strategies.

Disclosure Statement

Authors declare no conflicts of interest.

Abbreviations

ccRCC	clear cell renal cell carcinoma
DFS	disease-free survival
EMT	epithelial-to-mesenchymal transition
HIF	hypoxia-inducible factor
miRNA	microRNA
RCC	renal cell carcinoma
SKA1	spindle and kinetochore-associated protein 1
TKI	tyrosine kinase inhibitor
VEGF	vascular endothelial growth factor
VHL	von Hippel-Lindau

References

1 Capitanio U, Montorsi F. Renal cancer. *Lancet* 2016; **387**: 894–906.
2 Ferlay J, Soerjomataram I, Dikshit R *et al.* Cancer incidence and mortality worldwide: sources, methods and major patterns in GLOBOCAN 2012. *Int J Cancer* 2015; **136**: E359–86.
3 Rini BI, Campbell SC, Escudier B. Renal cell carcinoma. *Lancet* 2009; **373**: 1119–32.
4 Gnarra JR, Tory K, Weng Y *et al.* Mutations of the VHL tumour suppressor gene in renal carcinoma. *Nat Genet* 1994; **7**: 85–90.
5 Linehan WM, Rubin JS, Bottaro DP. VHL loss of function and its impact on oncogenic signaling networks in clear cell renal cell carcinoma. *Int J Biochem Cell Biol* 2009; **41**: 753–6.
6 Baldewijns MM, van Vlodrop IJ, Vermeulen PB, Soetekouw PM, van Engeland M, de Bruine AP. VHL and HIF signalling in renal cell carcinogenesis. *J Pathol* 2010; **221**: 125–38.
7 Kerbel RS. Tumor angiogenesis. *N Engl J Med* 2008; **358**: 2039–49.
8 Banumathy G, Cairns P. Signaling pathways in renal cell carcinoma. *Cancer Biol Ther* 2010; **10**: 658–64.
9 Sabatini DM. mTOR and cancer: insights into a complex relationship. *Nat Rev Cancer* 2006; **6**: 729–34.
10 Hsieh JJ, Purdue MP, Signoretti S *et al.* Renal cell carcinoma. *Nat Rev Dis Primers* 2017; **3**: 17009.
11 Philips GK, Atkins MB. New agents and new targets for renal cell carcinoma. *Am Soc Clin Oncol Educ Book* 2014; e222–7.
12 Duran I, Lambea J, Maroto P *et al.* Resistance to targeted therapies in renal cancer: the importance of changing the mechanism of action. *Target Oncol* 2017; **12**: 19–35.
13 Bartel DP. MicroRNAs: genomics, biogenesis, mechanism, and function. *Cell* 2004; **116**: 281–97.
14 Filipowicz W, Bhattacharyya SN, Sonenberg N. Mechanisms of post-transcriptional regulation by microRNAs: are the answers in sight? *Nat Rev Genet* 2008; **9**: 102–14.
15 Friedman RC, Farh KK, Burge CB, Bartel DP. Most mammalian mRNAs are conserved targets of microRNAs. *Genome Res* 2009; **19**: 92–105.
16 Nelson KM, Weiss GJ. MicroRNAs and cancer: past, present, and potential future. *Mol Cancer Ther* 2008; **7**: 3655–60.
17 Iorio MV, Croce CM. MicroRNAs in cancer: small molecules with a huge impact. *J Clin Oncol* 2009; **27**: 5848–56.
18 Esquela-Kerscher A, Slack FJ. Oncomirs - microRNAs with a role in cancer. *Nat Rev Cancer* 2006; **6**: 259–69.
19 Wiemer EA. The role of microRNAs in cancer: no small matter. *Eur J Cancer* 2007; **43**: 1529–44.
20 Kurozumi A, Goto Y, Okato A, Ichikawa T, Seki N. Aberrantly expressed microRNAs in bladder cancer and renal cell carcinoma. *J Hum Genet* 2017; **62**: 49–56.
21 Nakada C, Matsuura K, Tsukamoto Y *et al.* Genome-wide microRNA expression profiling in renal cell carcinoma: significant down-regulation of miR-141 and miR-200c. *J Pathol* 2008; **216**: 418–27.
22 Goto Y, Kurozumi A, Nohata N *et al.* The microRNA signature of patients with sunitinib failure: regulation of UHRF1 pathways by microRNA-101 in renal cell carcinoma. *Oncotarget* 2016; **7**: 59070–86.
23 National Institutes of Health: National Cancer Institute. The Cancer Genome Atlas (TCGA). [Cited 30 Apr 2017.] Available from URL: https://cancergenome.nih.gov/
24 Sobin LH, Gospodarowicz MK, Wittekind C. *International Union Against Cancer (UICC) TNM Classification of Malignant Tumors*, 7th edn. Oxford: Wiley-Blackwell, 2009.
25 Koshizuka K, Nohata N, Hanazawa T *et al.* Deep sequencing-based microRNA expression signatures in head and neck squamous cell carcinoma: dual strands of pre-miR-150 as antitumor miRNAs. *Oncotarget* 2017; **8**: 30288–304.
26 Goto Y, Kojima S, Kurozumi A *et al.* Regulation of E3 ubiquitin ligase-1 (WWP1) by microRNA-452 inhibits cancer cell migration and invasion in prostate cancer. *Br J Cancer* 2016; **114**: 1135–44.
27 Kurozumi A, Kato M, Goto Y *et al.* Regulation of the collagen cross-linking enzymes LOXL2 and PLOD2 by tumor-suppressive microRNA-26a/b in renal cell carcinoma. *Int J Oncol* 2016; **48**: 1837–46.
28 Okato A, Goto Y, Kurozumi A *et al.* Direct regulation of LAMP1 by tumor-suppressive microRNA-320a in prostate cancer. *Int J Oncol* 2016; **49**: 111–22.
29 Anaya J. OncoRank: A pan-cancer method of combining survival correlations and its application to mRNAs, miRNAs, and lncRNAs. *PeerJ Preprints* 2016; **1**(4): e2574.
30 Anaya J. OncoLnc: linking TCGA survival data to mRNAs, miRNAs, and lncRNAs. *PeerJ Computer Science* 2016; **2**: e67.
31 Gao J, Aksoy BA, Dogrusoz U *et al.* Integrative analysis of complex cancer genomics and clinical profiles using the cBioPortal. *Science Signaling* 2013; **6**(269): pl1.
32 Albiges L, Choueiri T, Escudier B *et al.* A systematic review of sequencing and combinations of systemic therapy in metastatic renal cancer. *Eur Urol* 2015; **67**: 100–10.
33 Calvo E, Schmidinger M, Heng DY, Grunwald V, Escudier B. Improvement in survival end points of patients with metastatic renal cell carcinoma through sequential targeted therapy. *Cancer Treat Rev* 2016; **50**: 109–17.
34 Lund AH. miR-10 in development and cancer. *Cell Death Differ* 2010; **17**: 209–14.
35 Khan S, Wall D, Curran C, Newell J, Kerin MJ, Dwyer RM. MicroRNA-10a is reduced in breast cancer and regulated in part through retinoic acid. *BMC Cancer* 2015; **15**: 345.
36 Ohuchida K, Mizumoto K, Lin C *et al.* MicroRNA-10a is overexpressed in human pancreatic cancer and involved in its invasiveness partially via suppression of the HOXA1 gene. *Ann Surg Oncol* 2012; **19**: 2394–402.
37 Jia H, Zhang Z, Zou D *et al.* MicroRNA-10a is down-regulated by DNA methylation and functions as a tumor suppressor in gastric cancer cells. *PLoS One* 2014; **9**: e88057.
38 Kowalik CG, Palmer DA, Sullivan TB *et al.* Profiling microRNA from nephrectomy and biopsy specimens: predictors of progression and survival in clear cell renal cell carcinoma. *BJU Int* 2017 (in press).
39 Goto Y, Kojima S, Nishikawa R *et al.* The microRNA-23b/27b/24-1 cluster is a disease progression marker and tumor suppressor in prostate cancer. *Oncotarget* 2014; **5**: 7748–59.
40 Inoguchi S, Seki N, Chiyomaru T *et al.* Tumour-suppressive microRNA-24-1 inhibits cancer cell proliferation through targeting FOXM1 in bladder cancer. *FEBS Lett* 2014; **588**: 3170–9.
41 Li Y, Chen D, Li Y *et al.* Oncogenic cAMP responsive element binding protein 1 is overexpressed upon loss of tumor suppressive miR-10b-5p and miR-363-3p in renal cancer. *Oncol Rep* 2016; **35**: 1967–78.
42 Guo Y, Lang X, Lu Z *et al.* MiR-10b directly targets ZEB1 and PIK3CA to curb adenomyotic epithelial cell invasiveness via upregulation of e-cadherin and inhibition of Akt phosphorylation. *Cell Physiol Biochem* 2015; **35**: 2169–80.
43 Hou R, Wang D, Lu J. MicroRNA-10b inhibits proliferation, migration and invasion in cervical cancer cells via direct targeting of insulin-like growth factor-1 receptor. *Oncol Lett* 2017; **13**: 5009–15.
44 Zhang B, Li KY, Chen HY *et al.* Spindle and kinetochore associated complex subunit 1 regulates the proliferation of oral adenosquamous carcinoma CAL-27 cells in vitro. *Cancer Cell Int* 2013; **13**: 83.
45 Qin X, Yuan B, Xu X, Huang H, Liu Y. Effects of short interfering RNA-mediated gene silencing of SKA1 on proliferation of hepatocellular carcinoma cells. *Scand J Gastroenterol* 2013; **48**: 1324–32.
46 Tian F, Xing X, Xu F *et al.* Downregulation of SKA1 gene expression inhibits cell growth in human bladder cancer. *Cancer Biother Radiopharm* 2015; **30**: 271–7.
47 Sun W, Yao L, Jiang B, Guo L, Wang Q. Spindle and kinetochore-associated protein 1 is overexpressed in gastric cancer and modulates cell growth. *Mol Cell Biochem* 2014; **391**: 167–74.
48 Li J, Xuan JW, Khatamianfar V *et al.* SKA1 over-expression promotes centriole over-duplication, centrosome amplification and prostate tumourigenesis. *J Pathol* 2014; **234**: 178–89.
49 Dong C, Wang XL, Ma BL. Expression of spindle and kinetochore-associated protein 1 is associated with poor prognosis in papillary thyroid carcinoma. *Dis Markers* 2015; **2015**: 616541.
50 Shen L, Yang M, Lin Q, Zhang Z, Miao C, Zhu B. SKA1 regulates the metastasis and cisplatin resistance of non-small cell lung cancer. *Oncol Rep* 2016; **35**: 2561–8.
51 Shi X, Chen X, Peng H *et al.* Lentivirus-mediated silencing of spindle and kinetochore-associated protein 1 inhibits the proliferation and invasion of neuronal glioblastoma cells. *Mol Med Rep* 2015; **11**: 3533–8.
52 Gaitanos TN, Santamaria A, Jeyaprakash AA, Wang B, Conti E, Nigg EA. Stable kinetochore-microtubule interactions depend on the Ska complex and its new component Ska3/C13Orf3. *EMBO J* 2009; **28**: 1442–52.
53 Schmidt JC, Arthanari H, Boeszoermenyi A *et al.* The kinetochore-bound Ska1 complex tracks depolymerizing microtubules and binds to curved protofilaments. *Dev Cell* 2012; **23**: 968–80.
54 Hanisch A, Sillje HH, Nigg EA. Timely anaphase onset requires a novel spindle and kinetochore complex comprising Ska1 and Ska2. *EMBO J* 2006; **25**: 5504–15.
55 Zhao LJ, Yang HL, Li KY *et al.* Knockdown of SKA1 gene inhibits cell proliferation and metastasis in human adenoid cystic carcinoma. *Biomed Pharmacother* 2017; **90**: 8–14.
56 Figlin RA, Kaufmann I, Brechbiel J. Targeting PI3K and mTORC2 in metastatic renal cell carcinoma: new strategies for overcoming resistance to VEGFR and mTORC1 inhibitors. *Int J Cancer* 2013; **133**: 788–96.
57 Siska PJ, Beckermann KE, Rathmell WK, Haake SM. Strategies to overcome therapeutic resistance in renal cell carcinoma. *Urol Oncol* 2017; **35**: 102–10.
58 Sakai I, Miyake H, Fujisawa M. Acquired resistance to sunitinib in human renal cell carcinoma cells is mediated by constitutive activation of signal transduction pathways associated with tumour cell proliferation. *BJU Int* 2013; **112**(2): E211–20.

Supporting Information

Additional Supporting Information may be found online in the supporting information tab for this article:

Fig. S1. Proliferation curves over time according to the results of XTT assays. (a) Transfection with *miR-10a-5p* in 786-O and A498 cells. (b) Transfection of si-*SKA1* into 786-O and A498 cells. (c) SKA1 rescue experiments. **P* < 0.001, ***P* < 0.0001.

Fig. S2. Phase micrographs of wound healing and invasion assays by transfection with *miR-10a-5p* in RCC cell lines. (a) Phase micrographs of 786-O and A498 cells 14 h after monolayer wound healing. (b) Phase micrographs of invading 786-O and A498 cells.

Fig. S3. Phase micrographs of wound healing and invasion assays by transfection with si-*SKA1* in 786-O cells. (a) Phase micrographs of 786-O cells 14 h after monolayer wound healing. (b) Phase micrographs of invading 786-O cells.

Fig. S4. Phase micrographs of wound healing and invasion assays by transfection with si-*SKA1* in A498 cells. (a) Phase micrographs of A498 cells 14 h after monolayer wound healing. (b) Phase micrographs of invading A498 cells.

Fig. S5. Phase micrographs of wound healing and invasion assays by cotransfection with *SKA1/miR-10a-5p* in 786-O cells. (a) Phase micrographs of 786-O cells 14 h after monolayer wound healing. (b) Phase micrographs of invading 786-O cells.

Fig. S6. Kaplan-Meier survival curves for disease-free survival rates based on expression of seven genes, excluding *SKA1*, in patients with ccRCC.

Figs S7–9. Expression levels of seven genes, excluding *SKA1*, according to TNM stage, T stage, and histological grade in patients with ccRCC from TCGA database. **P* < 0.01, ***P* < 0.001, ****P* < 0.0001.